The Structures of Two Hole Centers in the Mineral Brasilianite $NaAl_3(PO_4)_2(OH)_4$

K. D. Landrath and G. Lehmann

Institut für Physikalische Chemie der Westfälischen Wilhelms-Universität Münster

Z. Naturforsch. **42 a**, 572–576 (1987); received February 23, 1987

Two hole centers were detected in natural brazilianite by EPR at X-band and temperatures between 20 and 300 K. For the more intense center a hyperfine splitting (hfs) due to two nonequivalent Al nuclei could be completely analyzed by comparison of the hfs patterns with simulations for $1 \leqq A_1/A_2 \leqq 1.4$. The orientation of the principle axes of these hfs tensors allowed to assign this hole to a specific oxygen in the lattice. The phosphorus bound to it is evidently exchanged against a lower valency cation, most likely Si^{4+}. In the second center a hfs splitting due to one Al and one P nucleus was identified. Although a complete analysis of their hfs tensors was not possible, this center could also be assigned to a particular oxygen for which evidently one adjacent Al is exchanged against a divalent ion.

Introduction

Due to the intrinsic instability of the free O^{2-} ion a hole on an oxygen is by far the most frequent hole center in oxides. Its formation is normally caused by an adjacent cation impurity of lower valence than the host ion which also explains the relatively high thermal stability of this kind of centers which quite often can be observed in natural mineral specimens without additional irradiation treatment. The detailed determination of the structure of such radiation defects largely rests on the evaluation of the hyperfine splitting (hfs) of the neighboring atoms. The best known example of this kind is the smoky quartz center with dominating hfs due to an Al impurity [1–3]. In brazilianite hf interaction with the nucleus of at least one structural atom, either Al or P, can be expected, and in a previous study [4] an O^- adjacent to one Al and one P was postulated suggesting substitution of the second Al by a divalent impurity. Since the complete hfs tensors could not be evaluated, this interpretation was still tentative. A more detailed analysis of the spectra revealed, however, that in fact two largely overlapping centers were present. In the most intense one the hfs pattern is in fact caused by two largely inequivalent Al nuclei whereas the second center of lower intensity has the previously postulated structure. This is the first report of a complete analysis of the hfs tensors of two nonequivalent Al nuclei. Centers with an analogous structure and symmetry were detected in most feldspars [5–8]. Thus the method employed for analysis of the irregular shf patterns might find wider applications in the future and is thus of more general interest.

Reprint requests to Prof. Dr. G. Lehmann, Institut für Physikalische Chemie, Schlossplatz 4, D-4400 Münster.

Experimental

The same mineral specimens from Galilea Mine in Minas Geraes, Brazil, as in the previous study [4] were used. The easy cleavage plane (010) and the extensive striation along [001] facilitated their orientation. They were irradiated with X-rays (40 kV, 30 mA, copper anode) for 24 hours to increase the concentration of radiation defects and thus the signal/noise ratios.

The samples were rotated around the crystal axes b, c and a^* ($= b \times c$), and spectra were recorded in 2° intervals with a commercial X-band spectrometer B-ER 414 of Bruker Analytische Meßtechnik GmbH, Karlsruhe. A closed-cycle refrigeration system model CSA 202 of Air Products and Chemicals Inc., Alltentown, Pa., USA, allowed temperature regulation between 293 and about 20 K. The magnetic fields were determined with an AEG NMR Gaussmeter. and Picein (K. Roth, Karlsruhe) served as standard [8] for the determination of the microwave frequencies. The g-factors for the centers of gravity of the shf patterns in the rotational diagrams were fitted

0932-0784 / 87 / 0600-0572 $ 01.30/0. – Please order a reprint rather than making your own copy.

according to the method of Powell [9]. The hfs patterns were simulated in the range $1 \leqq A_1/A_2 \leqq 1.4$ for $A_1 + A_2 = 50$ MHz and $\Delta H_{pp} = 0.36$ mT assuming Lorentzian shape of the individual components. These patterns are thus characteristic for a ratio of separation to linewidth of 2.5.

Results

The quality of the spectra obtained at room temperature was not sufficient for the plotting of complete rotational diagrams. At about 55 K the individual linewidths reached their minimum values. Presumably due to partial saturation a further improvement was not possible below this temperature. As shown in Fig. 1, the spectra are due to two types of centers. The one of higher intensity with between 11 and 12 resolved hfs components will be called I in the following, the one of lower intensity (II) is only partly visible near $c \parallel B_0$ at high fields and near $a^* \parallel B_0$ at low fields. Both centers decay slowly near 500 K. Thus it was not possible to obtain one of them separately by a suitable thermal treatment. The rotational diagrams for rotations around the other axes c and a^* are more complex due to doubling of the spectra as expected for this space group with C_i as the only possible Laue point symmetry.

Center I

As shown in the example in Fig. 2, the intensities of the outer components of the shf pattern for the more intense center are always smaller than those of inner ones while the intensities for center II with comparable separations are constant within the limits of error. This suggests that in center I the shf pattern is caused by two Al while only one is involved in center II. The required mirror symmetries of these patterns were an additional aid for their analysis. The deviations from the intensity ratios of 1:2:3:4:5:6... calculated for two exactly equivalent Al nuclei can be ascribed to their inequivalence which varies with orientation. As shown in Fig. 3, the intensity ratio of the central to the outermost components decreases regularly with the ratio of their hfs constants A up to values of A_1/A_2 near 1.8. Above this value more than 11 components start to appear and thus it can be impossible to identify a central component in cases where the number of components is even.

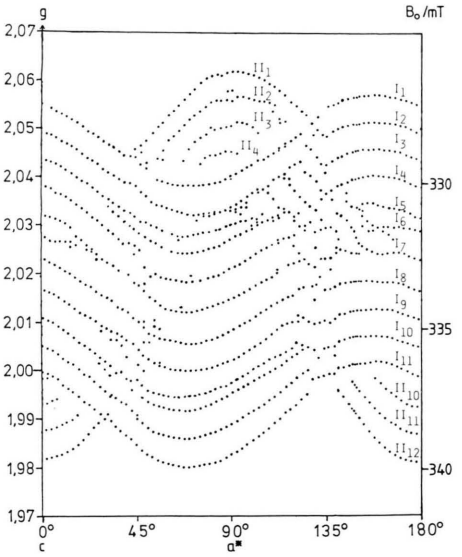

Fig. 1. Rotational diagram for the resolved hfs components of hole centers I and II for rotation around the crystal b axis at 9.42 GHz and 55 K.

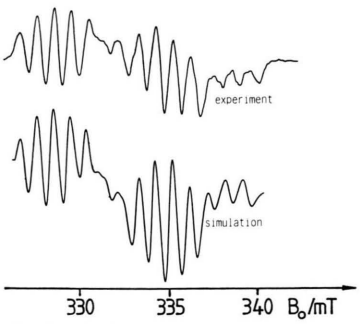

Fig. 2. EPR spectrum at 9.42 GHz and 55 K for $B_0 \parallel c$ (above) and simulation for $A_1/A_2 = 1.19$ for center I and $A_{Al} = 25.5$; $A_P = 98.1$ MHz for center II (below).

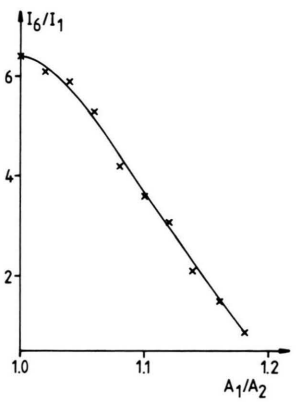

Fig. 3. Ratio of central to outer components of hfs multiplets for two nonequivalent nuclei with I = 5/2 each as a function of the ratio of their hfs constants determined from computer simulations.

Table 1. Principal values of the g matrix and the Al hfs tensors and their directions for center I.

	g	$\vartheta/°$*	$\varphi/°$	Direction in crystal	Deviation/°
1 g_{xx}	2.0300(7)	48.1(2.0)	73.9	Al(2) – P(2)	11.1
2 g_{yy}	2.0276	46.6	−138.4	Al(2) – O(7) – P(2) plane	31.0
3 g_{zz}	2.0022	73.4	− 31.6	Al(1) – O(7) – P(2) plane	33.1
		A_1 = Al(2)/MHz			
1 A_{xx}	30.8(4)	72(5)	4	Al(2) – O(7) – Al(2) plane	22.5
2 A_{yy}	29.6	130	78	⊥ Al(2) – O(7) – Al(2) plane	37.0
3 A_{zz}	25.9	135	−68	Al(2) – O(7)	6.9
		A_2 = Al(1)			
1 A_{xx}	25.0(4)	114(5)	−87	Al(1) – O(7) – Al(2) plane	13.3
2 A_{yy}	22.5	155	80	⊥ Al(1) – O(7) – Al(2) plane	21.1
3 A_{zz}	22.6	85	−0.5	Al(1) – O(7)	11.2

* ϑ and φ are the angles to the crystal b and c axes resp.

Table 2. Principal values of g matrix, their directions and approximate hfs data for center II.

	g	$\vartheta/°$	$\varphi/°$	Direction in crystal	Deviation/°
1 g_{xx}	2.0363(7)	87.7(3.0)	5.4	Al(3) – P(1)	15.8
2 g_{yy}	2.0224	107.4	94.3	Al(3) – O(6) – P(1) plane	18.8
3 g_{zz}	2.0024	17.6	102.7	⊥ Al(3) – O(6) – P(1) plane	11.9

$A_{zz} \approx 23$ MHz (close to a^* axis); $A_{xx} \approx A_{yy} \approx 25.5$ MHz (Al(3)); $A \approx A_{iso} \approx 98$ MHz (P(1)).

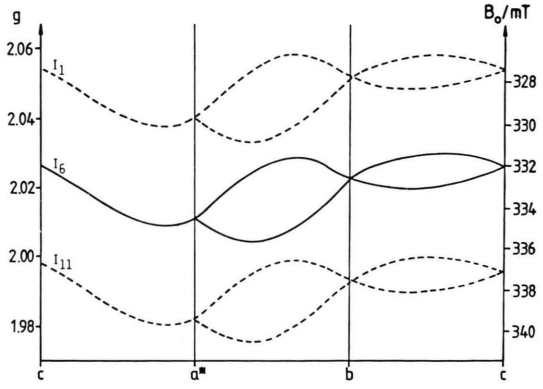

Fig. 4. Angular variation of the center of gravity and the outer hfs components for rotations around the b, c and a^* axes at 9.42 GHz and 55 K for center I.

Nevertheless, the patterns are quite characteristic for a particular ratio, and thus it can be determined unambigously by comparison with these simulations and furthermore it is possible to subtract the contribution of center II and analyze it separately. The absolute values of the shf constants A_i can then be obtained from the total spread of the shf patterns. In Fig. 4 the rotational diagrams of the g factors and of the outermost hfs components for center I are plotted. The principal values of the g matrix and A tensor for center I and their orientations with respect to the crystal axes system are listed in Table 1. Since $A_1 > A_2$ at all orientations, it is not surprising that no hfs pattern with the intensity ratios expected for two Al nuclei can be observed which caused misinterpretation of the structure of this center in the previous study [4].

Center II

The analysis of the hfs patterns clearly showed that this center consists of two hfs sextets. Thus a nucleus with $I = 1/2$ must be present in addition to one Al, and for reasons to be discussed later only P is a possible candidate. Rotational diagrams similar to those for center I in Fig. 2 were obtained for this center also. The hfs multiplets showed a minimum spread of about 7.6 mT near a^* and maximum values near 8.0_5 mT near b and c and separations of the individual components near 25.5 MHz along b and c. Since the anisotropy of the hfs splitting due to ^{31}P in a PO_4^{2-} unit is very small [11], the variation in this total spread of the hfs structure can be attributed to the anisotropy of the ^{27}Al hfs. This results in the approximate hfs data listed in Table 2 together with the principal values of the g matrix and their orientations.

Discussion

According to the principal values of their g matrices, both centers clearly are of the hole type, and the deviations from the g factor of a free electron suggest that in first approximation these holes are localized in a $2p$ level of two different oxygens. It should be possible to identify these oxygens from the orientations of the principal values relative to bond directions of the different oxygens. Analysis of the hfs anisotropy generally is most straightforward as long as nearly axial tensors are found. The strong localization of the holes on particular oxygens, evident from the small increase of the EPR linewidths up to room temperature, is a further aid to check these results. As shown in several cases, e.g. the smoky quartz center [2], the oxygen with the longest bond distance to the lower valence impurity ion is always energetically preferred. Thus the fairly large distortions of the PO_4 and AlO_6 units in brazilianite [10] cause this localization and evidently also the lack of any optical absorption due to these centers in the visible range [4].

Center I

In Table 1 the orientations of the principal values of the g matrix and Al hfs tensors for center I are compared to selected bond distances in brazilianite, and Fig. 5 shows them in a stereographic projection. The directions of A_{zz} for Al(1) and Al(2) suggest that the hole is localized on oxygen O(7) which is bound to Al(1), Al(2) and P(2) [10]. Since no hfs due to a P nucleus can be detected, P(2) must be exchanged against a lower valence cation, and Si is the most likely candidate. The signal/noise ratios were too low to observe hfs satellites due to ^{29}Si of only 2.4% the intensity of the main signals. Indeed P(2) – O(7) is the largest bond distance of 155.8 pm in this PO_4 group, the distances to O(6) and O(12) are 1.8 pm shorter. Comparison with the bond length difference of the SiO_4 groups in quartz [12] together with the energy difference of 30 meV for the excited and ground state of the smoky quartz center [1] suggests that at room temperature only about 2% of the holes in center I should be raised into the excited states, again too low a proportion to be observable. In the PO_4 unit of P(1) the P(1) – O(6) distance of 156.4 pm is even larger, but A_{zz} is almost perpendicular to Al(3) – O(6), the shorter one of the two Al – O(6) bond distances. Thus this oxygen can be excluded for center I.

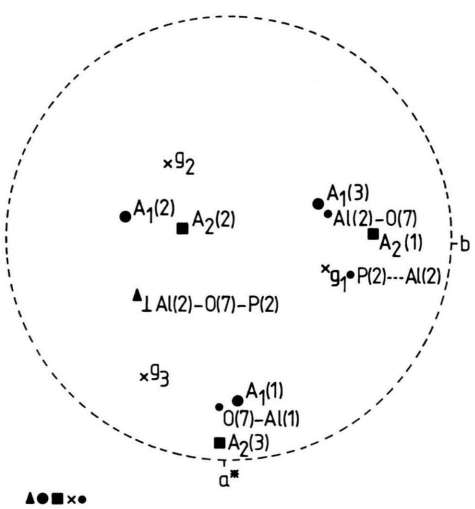

Fig. 5. Stereographic projection of the principal directions of the g matrix and A_{Al} tensors for center I and of selected bond directions in brazilianite. Due to the presence of two magnetically nonequivalent sites an equivalent set of directions symmetrical to the a^* axis is also present.

From the directions of the principal values of the g matrix the orientations of the 2 p levels of the O^- can be determined with $g_{zz} \approx g_{free}$ indicating the direction of the 2 p_z orbital in which most of the unpaired spin density is localized. It is nearly oriented along the line joining Al(1) and Al(2) and thus far (59°) away from the Al(2)–O(7) direction. Such an orientation cannot lead to a significant isotropic hfs due to the s-electron density on Al(2), and thus the (negative) value of A_{iso} must be caused by exchange polarization [13], just as in the case of the smoky quartz center where this p_z orbital is nearly perpendicular to the O – Al direction [2].

Since the hfs from the second Al is always smaller, this must be the one with significantly longer bond distance to O(7). With Al(2) – O(7) = 200.2 and Al(1) – O(7) = 211.9 pm this condition is indeed fulfilled. The direction Al(1) – O(7) is close to $A_2(3)$ which thus has to be identified with A_{zz} for Al(1). Although this is much closer to the direction of g_{zz}, again a negative value of A_{iso} compatible only with exchange polarization and a three times larger rhombic component C than the axial B result. Calculation of the relaxed Al – O bond distances from the anisotropic hfs data based on a purely electrostatic model [14] have in the past been

attempted, but led to unrealistically large elongations for the smoky quartz center of 40% [2]. Thus, once again the exchange polarization mechanism appears to lead to more reliable values, but most likely the changes in this case are not much larger than the present uncertainty of this model.

Center II

With A_{zz} for the Al nucleus very nearly aligned along the a^*-axis and an approximately axial tensor, it should also be possible to locate the oxygen on which this hole is localized. Since a hole on an OH group is less stable, and furthermore a highly anisotropic hfs should result from a neighboring proton, only ^{31}P remains as the cause of the doublet splitting thus eliminating the four hydroxyl oxygens. The value of A(P) near 100 MHz estimated from the incomplete hfs data also fits well into the range of data for other PO_4^{2-} units between 54 MHz for calcite and 126 MHz for α-quartz [11]. Since only the Al(3) – O(6) direction is close to the a^*-axis as shown in the stereographic projection in Fig. 6, Al(2) must then be substituted by a divalent ion (either Mg or Zn according to the trace analyses [4]). Al(2) – O(6) is the longest bond distance of 210.7 pm in this AlO_6 unit. Also, the average Al – O bond distance (excluding the normally longer OH bonds) is by far largest for Al(2) [10], and this should strongly favor preferential substitution of this Al by the larger divalent cations. Since g_{zz} is nearly perpendicular to the Al(3) – O(6) direction (and the Al(3) – O(6) – P(1) plane) it is not surprising

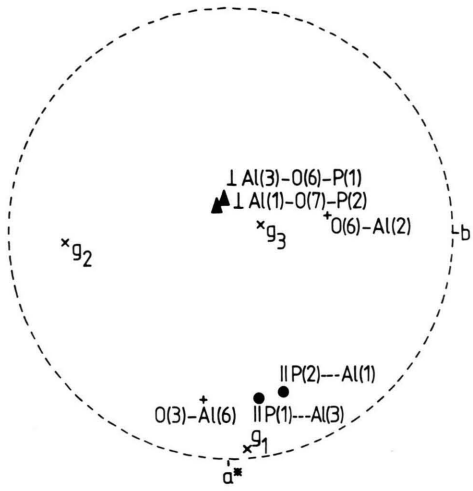

Fig. 6. Stereographic projection of the principal directions of the g matrix for center II and of selected bond directions in brazilianite.

that once again a negative value of the isotropic hfs splitting constant due to exchange polarization is obtained. Its value is intermediate between those for center I and thus also correlates well with the lengths of the Al – O bonds associated with them. Thus a completely consistent interpretation of all results for both centers could be obtained.

Acknowledgement

Financial support of the essential computer part of this work by the Fonds der Chemischen Industrie is gratefully acknowledged.

[1] R. Schnadt and J. Schneider, Phys. kondens. Materie **11,** 19 (1970).
[2] R. D. H. Nuttall and J. A. Weil, Can. J. Phys. **59,** 1696 (1981).
[3] R. B. Bossoli and L. E. Halliburton, phys. stat. sol. **B 136,** 709 (1986).
[4] A. Requardt, F. Hill, and G. Lehmann, Z. Naturforsch. **37 a,** 280 (1982).
[5] V. A. Ioffe and I. S. Yanchevskaya, Sov. Phys. Sol. State **10,** 370 (1968).
[6] A. S. Marfunin and L. V. Berhov, Dokl. Acad. Nauk SSSR **193,** 412 (1970).
[7] B. Speit and G. Lehmann, Phys. Chem. Minerals **8,** 77 (1982).
[8] M. J. D. Powell, Comp. J. **7,** 155 (1964).
[9] B. Schmitz, M. Jakubith, and G. Lehmann, Z. Naturforsch. **34 a,** 906 (1979).
[10] B. M. Gatehouse and B. K. Miskin, Acta Crystallogr. **B 30,** 1311 (1974).
[11] see, e.g. D. Maschmeyer and G. Lehmann, Z. Kristallogr. **163,** 181 (1983) and the references cited in Table 3 of this work.
[12] Y. Le Page and G. Donnay, Acta Crystallogr. **B 32,** 2456 (1976).
[13] F. J. Adrian and A. N. Jette, J. Chem. Phys. **81,** 2416 (1984); F. J. Adrian, A. N. Jette, and J. M. Spaeth, Phys. Rev. **B 31,** 3923 (1985).
[14] O. F. Schirmer, J. Phys. Chem. Solids **29,** 1407 (1968).